



Proceedings Article

A receive insert for non-human primate functional MPI (fMPI)

Jorge Chacon-Caldera ^{a,b,*} · Eli Mattingly^{a,c,d} · Monika Śliwiak ^a · Alex C. Barksdale^{a,d} · Frauke H. Niebel^{a,e,f} · Lawrence L. Wald^{a,b,c}

^a Martinos Center for Biomedical Imaging, Massachusetts General Hospital, Charlestown, MA, USA

^b Harvard Medical School, Boston, MA, USA

^c Harvard-MIT Division of Health Sciences & Technology, Cambridge, MA, USA

^d Massachusetts Institute of Technology, Cambridge, MA, USA

^e Fraunhofer Research Institution for Individualized and Cell-Based Medical Engineering IMTE, Lübeck, Germany

^f Institute of Medical Engineering, University of Lübeck, Lübeck, Germany

*Corresponding author, email: jchaconcaldera@mgh.harvard.edu

© 2024 Chacon-Caldera *et al.*; licensee Infinite Science Publishing GmbH

This is an Open Access article distributed under the terms of the Creative Commons Attribution License (<http://creativecommons.org/licenses/by/4.0>), which permits unrestricted use, distribution, and reproduction in any medium, provided the original work is properly cited.

Abstract

We designed and built a receive gradiometer coil for non-human primate (NHP) fMPI studies. The coil was integrated and tested within our human-size brain MPI system. We demonstrate the imaging resolution and sensitivity expected in NHP studies using a dilution series sensitivity measurement (120 μg to 23 ng iron mass) and a NHP-brain-sized phantom with an iron concentration of 62.5 $\mu\text{g}/\text{ml}$, below the level expected in arterial blood in MPI (143.0 $\mu\text{g}/\text{ml}$). Using 6 mT drive amplitudes and producing one 12.8 cm field-of-view image every 4.7 seconds resulted in a detection limit (SNR = 1) of 19.5 ng of iron in 2D imaging and good image quality. This would correspond to a contrast-to-noise ratio (CNR) of ~ 20 for a 25% change of cerebral blood volume (CBV) following activation in a 6 mm isotropic voxel. These promising preliminary sensitivity levels encourage the pursuit of the first in vivo brain function MPI experiments in primates.

1. Introduction

Functional brain studies spatially map the brain activation associated with a given activity or task. However, the task-induced hemodynamic changes observed in fMRI are weak and studying them typically requires averaging large cohorts of subjects to achieve statistical significance. Subject averaging compensates for the low CNR (~ 5 in fMRI) [1] but it is notoriously problematic due to the differences in brain folding patterns among individuals [2]. Perhaps more importantly, clinical use of the method requires abnormal patterns to be detected in an individual.

A previous study using a small bore MPI imager to

perform fMPI in rodents showed up to 6 \times higher CNR than fMRI [3]. However, rodents have much smaller and less complex brains than primates.

Dedicated receive coils have already demonstrated increased sensitivity in previous MPI studies [4, 5]. This suggests that a receive insert that can tightly fit the head of non-human primates could boost CNR in fMPI compared to using a human receive coil due to a higher fill factor.

Here, we present a receive insert for non-human primates, evaluated in our in-house-built human-brain-sized MPI system.

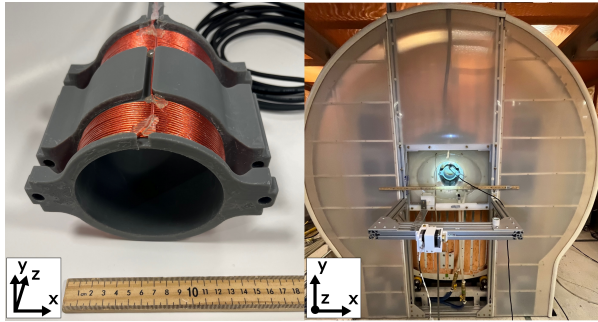


Figure 1: Photograph of the receive insert for non-human primates (left) and integrated in our MPI system (right).

II. Material and methods

The insert was designed as a linear gradiometer receive coil. The holder was 3D printed with grey resin V4 FLGPGR04 material (Formlabs Inc., Somerville, MA, USA) with an inner diameter of 11 cm. In each half we wound 17 turns of type-2 Litz wire with 115 strands, 36 AWG and PFA coating (New England Wire Technologies, Lisbon, NH, USA). The gradiometer was connected to our receive filter via an XLR cable of 5.5 m in length (see Figure 1), yielding an inductance of 83.5 μH for the coil and the cable.

The gradiometer was connected to a purpose-built 4th-order band-stop filter to attenuate the feedthrough of the fundamental harmonic of the drive field. The filter included a 1:5 output transformer. The differential output of the filter was connected to a pre-amplifier based on the AD8429 low noise instrumentation amplifier (Analog Devices, Wilmington, MA, USA), with an expected noise performance of $\sim 1 \text{ nV}/\sqrt{\text{Hz}}$. Finally, the signal harmonics (2nd to 9th) were digitized in differential mode using a PXIe-6361, X series DAQ (National Inst., Austin, TX, USA).

For imaging, we used our in-house-developed human-brain-sized MPI scanner. The scanner has an FFL topology with $G_z \approx 0.85$ and $G_{x'} \approx 1.13 \text{ T/m}$, where the z-axis is parallel to the drive field, and the x' -axis is a mechanically rotating axis perpendicular to the drive and FFL axes. The translation of the FFL across the head is achieved with electromagnet "shift" coils. Our imaging frequencies were: drive = 26.3 kHz sine, shift = 2.85 Hz triangle, and rotation = 0.11 Hz. This yielded one image per 180° gantry rotation, which occurs every 4.74 seconds. The drive field amplitude was chosen to be 6 mT_{pk} requiring 50 A_{pk} in the human-sized drive coil.

The dilution series utilized dot phantoms containing a volume of 20 μl of 50 nm diameter Synomag COOH (Die micromod Partikeltechnologie GmbH, Rockstock, Germany). The concentrations were successively decreased by dilution with distilled water. The following iron masses were tested: 120, 43, 23, 11, 7, 3, 1.4, 0.727,

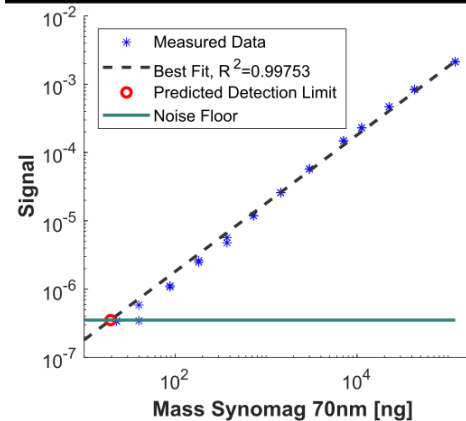
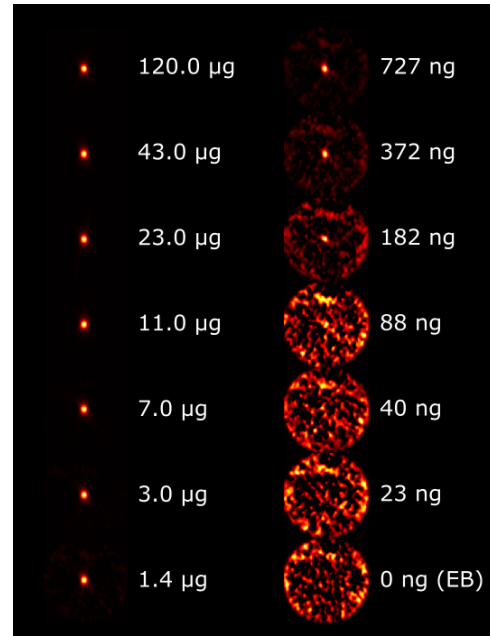


Figure 2: Dilution series and detection limit using the receive insert. Top: Imaging of 20 μl dot phantoms with different iron masses. Bottom: Signal amplitudes at the pixel location with maximum intensity in the 120 μg image versus iron mass. The predicted limit of detection is 19.5 ng.

0.372, 0.182, 0.088, 0.040, and 0.023 μg , as well as empty bore (EB).

The imaging capabilities of our NHP MPI system were demonstrated with a phantom of the letter M, comparable in size to the rhesus macaque brain. The letter had a 4 mm font thickness and 4 mm of depth. It covered a maximum distance of 81 mm e.g. from top-left corner to bottom-right corner. The phantom was filled with 70 nm diameter Synomag-D particles (Die micromod Partikeltechnologie GmbH, Rockstock, Germany). We used a concentration of 62.5 $\mu\text{g}/\text{ml}$, which is lower than the iron concentration expected in the NHP's arterial blood (143 $\mu\text{g}/\text{ml}$ for a NHP bolus of 100 mg in 0.7 L of blood), or the 80 $\mu\text{g}/\text{mL}$ expect in human arterial blood at human dose levels [1].

II.I. Reconstruction and Data Processing

Our reconstruction pipeline included the subtraction of a single empty bore measurement collected at the end of our dilution series. For the M-phantom no empty bore subtraction was used. From these data, a 2D sinogram was filled for each dataset by mapping the amplitude of the 3rd harmonic to 132 instantaneous locations and 27 angles of the FFL. Each sinogram was then transformed into image space by using a filtered-back-projection with a Ram-Lak filter. The resulting image was convolved with a 6-mm Gaussian filter, corresponding to the native in-plane resolution of our imager.

We estimated the limit of detection of our system from our dilution series by linearly fitting the signal amplitude of the 4.7 s images. This was performed in the same pixel location in all images after selecting the location with the maximum signal amplitude in the 120 μg image. The noise floor was determined from the empty bore image. We assumed our limit of detection at $\text{SNR} = 1$ from the intersection of the linear fit and the noise floor. Data from two different images for each iron mass were tested separately.

III. Results and discussion

Figure 2 shows the dilution series images. The SNR allowed to detect masses up to 182 ng without effort with the naked eye. The slope of the signal amplitudes fit the linear scaling of the iron mass well ($R^2 = 0.998$). This is true for both images acquired at each iron mass in the series. From the fitted line, the $\text{SNR} = 1$ detection limit was 19.5 ng.

Comparing to other MPI systems with different topologies is not straightforward, but our rodent MPI system used a nearly identical topology. The smaller rodent system and coils yielded a ~ 15 -fold better sensitivity using a 8 mT_{pk} drive [6], mainly due to the higher drive amplitude and smaller Rx coil size. The larger voxel volumes (6 mm isotropic voxel for the human instrument compared to 3 mm isotropic for the rodent scanner) will provide 8 \times more iron mass in the NHP imaging voxels. Together we expect to visualize the NHP functional activation with a $\text{CNR} \approx 20$ (25% CBV change in a 6 mm isotropic voxel with 5% blood).

Figure 3 shows the design and dimensions of the scanned M-phantom and the reconstructed image. Good image quality can be observed, albeit with some artifacts, especially in the corners where the straight lines appear bent. We attribute this effect to the basic reconstruction used, which does not account for field and trajectory imperfections. Another contributing factor could be the discretization of the FFL's dynamically continuous position and angle. A more detailed analysis of the source and mitigation of these artifacts, as well as achievable spatial resolution is in the scope of our future work.

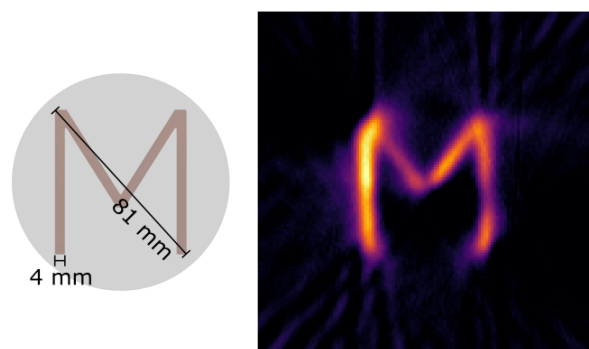


Figure 3: Model of the M-phantom and imaging. The phantom has a depth of 4 mm and an iron concentration of 62.5 $\mu\text{g}/\text{ml}$, lower than the non-bolus iron concentration expected in the NHP's arterial blood (143 $\mu\text{g}/\text{ml}$).

Another caveat in our reconstruction pipeline is that only 2D imaging is performed. However, implementing pipelines for 3D reconstructions and other deconvolution techniques based on system-matrix approaches [7–9] is possible. These methods could allow volumetric reconstructions at the cost of added noise due to the deconvolution operation. Despite these drawbacks, our system demonstrated large field-of-view imaging capabilities in our current implementation. We expect further optimizations and tests to enable in vivo fMPI measurements using non-human primates in the near future.

IV. Conclusions

In this work we built and evaluated an insert for non-human primate fMPI studies. Our system demonstrated good preliminary sensitivity and adequate field-of-view for enabling fMPI imaging of CBV changes associated with neuroactivation in non-human primates.

Acknowledgments

Funding was provided by the National Institute of Biomedical Imaging and Bioengineering (NIBIB), of the National Institutes of Health (NIH) under award numbers 5T32EB1680, U01EB025121, and NSF GRFP 1122374.

Author's statement

Conflict of interest: Authors state no conflict of interest.

References

- [1] E. E. Mason, C. Z. Cooley, S. F. Cauley, M. A. Griswold, S. M. Conolly, and L. L. Wald. Design analysis of an mpi human functional brain scanner. *International journal on magnetic particle imaging*, 3(1), 2017.
- [2] B. Fischl, M. I. Sereno, R. B. Tootell, and A. M. Dale. High-resolution intersubject averaging and a coordinate system for the cortical surface. *Human brain mapping*, 8(4):272–284, 1999.
- [3] E. E. Mason, E. Mattingly, K. Herb, S. F. Cauley, M. Śliwiak, J. M. Drago, M. Graeser, E. T. Mandeville, J. B. Mandeville, and L. L. Wald. Functional magnetic particle imaging (fmpi) of cerebrovascular changes in the rat brain during hypercapnia. *Physics in Medicine & Biology*, 68(17):175032, 2023.
- [4] H. Paysen, J. Wells, O. Kosch, U. Steinhoff, J. Franke, L. Trahms, T. Schaeffter, and F. Wiekhorst. Improved sensitivity and limit-of-detection using a receive-only coil in magnetic particle imaging. *Physics in Medicine & Biology*, 63(13):13NT02, 2018.
- [5] M. Graeser, P. Ludewig, P. Szwargulski, F. Foerger, T. Liebing, N. D. Forkert, F. Thieben, T. Magnus, and T. Knopp. Design of a head coil for high resolution mouse brain perfusion imaging using magnetic particle imaging. *Physics in Medicine & Biology*, 65(23):235007, 2020.
- [6] E. Mattingly, E. E. Mason, K. Herb, M. Śliwiak, J. Drago, M. Graeser, and L. L. Wald. A sensitive, stable, continuously rotating ffl mpi system for functional imaging of the rat brain. *Int. J. Magn. Part. Imaging*, 8:2212001, 2022.
- [7] E. E. Mason, S. F. Cauley, E. Mattingly, M. Sliwiak, and L. L. Wald. Side lobe informed center extraction (slice): A projection-space forward model reconstruction for a 2d imaging system. *International Journal on Magnetic Particle Imaging IJMPI*, 8(1 Suppl 1), 2022.
- [8] J. Chacon-Caldera, H. Lehr, K. Sajjamark, and J. Franke. Eigenreconstructions: A closer look into the system matrix. *International Journal on Magnetic Particle Imaging IJMPI*, 6(2 Suppl 1), 2020.
- [9] J. Chacon-Caldera, H. Lehr, K. Sajjamark, and J. Franke. Enhancing spatial resolution in magnetic particle imaging using eigenreconstructions: Opportunities and limitations. *International Journal on Magnetic Particle Imaging IJMPI*, 7(2), 2021.